Uncovering a Calcium-Regulated Membrane-Binding Mechanism for Soybean Lipoxygenase-1†

Suren A. Tatulian,*,‡ Janusz Steczko,§,|| and Wladek Minor‡

Department of Molecular Physiology and Biological Physics, University of Virginia School of Medicine, P.O. Box 10011, Charlottesville, Virginia 22906-0011, and Institute of Catalysis and Surface Chemistry, Polish Academy of Sciences, 30239 Krakow, Poland

Received May 7, 1998; Revised Manuscript Received September 9, 1998

ABSTRACT: Lipoxygenases catalyze the biosynthesis of leukotrienes, lipoxins, and other lipid-derived mediators that are involved in a wide variety of pathophysiological processes, including inflammation, allergy, and tumorigenesis. Mammalian lipoxygenases are activated by a calcium-mediated translocation to intracellular membranes upon cell stimulation, and cooperate with cytosolic phospholipase A_2 at the membrane surface to generate eicosanoids. Although it has been documented that plant cell stimulation increases intracellular Ca^{2+} concentration and activates cytosolic phospholipase A_2, followed by lipoxygenase-catalyzed conversion of the liberated linolenic acid to jasmonic acid, no evidence is available for Ca^{2+}-regulated membrane binding and activity of plant lipoxygenases. Plant lipoxygenases, unlike their mammalian counterparts, are believed to function independently of calcium or membranes. Here we present spectroscopic evidence for a calcium-regulated membrane-binding mechanism of soybean lipoxygenase-1 (L-1). Both calcium and membrane binding affect the structure and the mode of action of L-1. Free L-1 in solution is less accessible to the polar solvent and converts linoleic acid to conjugated dienes, whereas surface binding increases solvent accessibility and stimulates conjugated ketodiene production. Calcium exerts a biphasic effect on the structure and activity of L-1. Our results uncover a new regulatory mechanism for plant lipoxygenases and delineate common features in animal and plant cell signaling pathways.

In several experimental settings, stimulation of animal cells is followed by activation of cytosolic phospholipase A_2 (PLA_2[1]), which transiently binds to intracellular membranes in a Ca^{2+}-dependent manner and cleaves arachidonic and other fatty acids from membrane lipids (*1*, *2*). Subsequent oxygenation of arachidonic acid by lipoxygenases (LOX), cyclooxygenases, or cytochrome P450 leads to the biosynthesis of eicosanoids that play significant roles in many pathophysiological processes (*3*−*8*). LOX metabolites of arachidonic acid, namely leukotrienes and lipoxins, are potent mediators of inflammatory and allergic disorders, including inflammatory bowel disease, glomerulonephritis, rheumatoid arthritis, asthma, and atherogenesis (*3*, *9*−*17*). Moreover, results of recent research on leukemia and lung, prostate, and breast cancer strongly imply that LOX products, especially those of 5- and 12-LOXs, stimulate certain oncogenes and downregulate the apoptosis of malignant cells, thus increasing their metastatic potential (*18*−*21*). There is strong evidence that mammalian 5-LOX is activated by a Ca^{2+}-mediated translocation to the nuclear envelope upon cell stimulation and by interaction with the 5-lipoxygenase-activating protein (5-LAP), a nuclear membrane integral protein that binds arachidonic acid (*22*−*24*). Partitioning of 5-LOX is paralleled by a similar translocation of the cytosolic PLA_2 to the nuclear envelope (*24*). This leads to an interesting scenario of a cooperation between the three proteins at the membrane surface, that is, liberation of arachidonate by PLA_2 and its delivery to the 5-LOX by 5-LAP. A Ca^{2+}-mediated binding to intracellular membranes during cell stimulation has also been demonstrated for mammalian 12- and 15-LOXs (*25*, *26*). These enzymes also bind to artificial lipid bilayers in a Ca^{2+}-dependent manner (*26*, *27*).

In plant cells, LOXs act on linoleic and linolenic acids to produce the multifunctional phytohormone jasmonic acid and other mediators (*28*, *29*). Although it has been documented that plant cell stimulation by elicitors and other agents increases intracellular Ca^{2+} concentration and activates cytosolic PLA_2 among other signaling molecules, which is followed by LOX-catalyzed conversion of the liberated linolenic acid to jasmonic acid (*30*−*33*), no evidence is

† Supported in part by a grant from American Heart Association to S.A.T. (96−1364). J.S. was supported in part by an International Research Scholarship award from the Howard Hughes Medical Institute (HHMI 77195-543901).

* Corresponding author. Telephone: (804) 982-3855. Fax: (804) 982-1616. E-mail: st8m@virginia.edu.

‡ University of Virginia School of Medicine.

§ Polish Academy of Sciences.

|| Present address: HemoCleanse Inc., Purdue Research Park, West Lafayette, Indiana 47906.

[1] Abbreviations: ATR, attenuated total reflection; DOPC, dioleoylphosphatidylcholine; DPE, *N*-dansyl-phosphatidylethanolamine; FRET, fluorescence resonance energy transfer; FTIR, Fourier transform infrared; L-1, soybean lipoxygenase-1; LA, linoleic acid; 5-LAP, 5-lipoxygenase-activating protein; LOX, lipoxygenase; PLA_2, phospholipase A_2; PLPC, 1-palmitoyl-2-linoleoylphosphatidylcholine; POPC, 1-palmitoyl-2-oleoylphosphatidylcholine; POPS, 1-palmitoyl-2-oleoylphosphatidylserine.

10.1021/bi981062t CCC: $15.00
Published on Web 10/16/1998

available for Ca^{2+}-regulated membrane binding and activity of plant LOXs.

Lipoxygenases are single-chain, non-heme, iron-containing enzymes. The soybean isozyme L-1 is the first LOX which has been purified to homogeneity (*34*, *35*) and whose atomic resolution crystal structure has been determined by X-ray crystallography (*36*, *37*). This is a 839-residue protein composed of two major structural domains, the N-terminal 8-stranded antiparallel β-barrel domain with yet unidentified function (residues 1−146) and the C-terminal catalytic, mostly α-helical domain containing the ligands for the iron cofactor. The crystal structure of soybean L-3 isozyme revealed a similar 3-dimensional fold, despite different positional specificity of fatty acid hydroperoxidation by L-1 and L-3 (*38*). Plant and mammalian LOXs share only 21%−27% sequence identity; the most significant primary structure differences are found in the N-terminal region. This, together with the fact that mammalian LOXs are shorter than the plant enzymes (662−674 and 839−923 residues, respectively), has led many researchers to assume that the N-terminal β-barrel is absent in mammalian LOXs (*39*, *40*). However, the X-ray structure of the rabbit 15-LOX uncovered an N-terminal 115-residue antiparallel β-barrel domain (*41*), predicting similarities in the molecular mechanisms of plant and animal LOXs in addition to the common chemical mechanism of catalysis.

Before the discovery of iron in LOXs, several studies were undertaken to establish a role for Ca^{2+} in the activity of plant LOXs. Calcium increased the activity of the navy bean LOX (*42*) and the soybean L-2 isozyme (*43*), inhibited the soybean L-3 isozyme (*44*), and had a biphasic effect on the horse bean LOX activity (*45*). After the discovery of iron in LOXs, the interest in calcium diminished and the role of Ca^{2+} ions in LOX activity has remained a "subject of considerable controversy" (*28*). Although the soybean L-2 enzyme (*46*) and a specific "lipid body" LOX found in cucumber cotyledons (*47*) are able to attack membrane lipids and oxygenate esterified fatty acids, plant LOXs are believed to function independently of membranes or Ca^{2+} ions. Here we demonstrate that soybean lipoxygenase L-1 binds to phospholipid bilayers and that Ca^{2+} exerts significant effects on the membrane binding, structure, and mode of action of this enzyme. We further provide evidence that the N-terminal β-barrel domain of L-1 is likely involved in the interaction of the enzyme with membranes.

EXPERIMENTAL PROCEDURES

L-1 was expressed in *Escherichia coli* and purified as described (*48*). The purified protein was stored in 50 mM phosphate buffer, pH 5.6, at −70 °C and was transferred to a desirable buffer of pH 8−9 immediately before measurements using Centricon-30 concentrators (Amicon, Beverly, MA). The secretory PLA_2 has been purified according to Maraganore et al. (*49*) from the venom of the snake *Agkistrodon piscivorus piscivorus*, and was a gift from Dr. R. L. Biltonen of the Department of Pharmacology, University of Virginia Medical School. The lipids were from Avanti Polar Lipids (Alabaster, AL), and other chemicals were from Sigma (St. Louis, MO). Protein concentration was determined by Bradford assay (*50*). Oxygen concentration was calibrated by bubbling the buffers with O_2 or N_2 and measured by an ISO_2 dissolved oxygen meter (World Precision Instruments, Sarasota, FL). Low calcium concentrations were adjusted by EGTA and calculated using an EGTA-Ca^{2+} affinity constant $\log K = 6.389 + 1.98(\mathrm{pH} - 7)$, following the procedures described by Bers et al. (*51*). Lipid vesicles were prepared either by sonication of the suspensions using a tip ultrasonifier or by extrusion through 100 nm pore size polycarbonate membranes (Nucleopore, Pleasanton, CA) using a Liposofast extruder (Avestin, Ottawa, Canada).

Transmittance and attenuated total reflection (ATR) Fourier transform infrared (FTIR) experiments were carried out on a Nicolet 740 spectrometer (Nicolet Analytical Instruments, Madison, WI), as described (*52*). In transmittance FTIR experiments, a precision liquid cell with CaF_2 windows was used (Buck Scientific, East Norwalk, CT). Supported bilayers on $1 \times 20 \times 50$ mm^3 germanium internal reflection plates (Buck Scientific) were prepared by deposition of a phospholipid monolayer onto the plate, using a Langmuir−Blodgett monolayer trough (Mayer, Göttingen, Germany). The plate with the monolayer was assembled in an ATR cell, and then extruded phospholipid vesicles were injected into the cell and incubated for ∼1 h at room temperature to allow the vesicles to spread on the monolayer, yielding supported phospholipid bilayers. Samples for FTIR experiments were prepared in D_2O buffers, and pD was calculated as $\mathrm{pD} = \mathrm{pH}^* + 0.4$, where pH* is the pH meter reading. FTIR experiments were performed at 2 cm^{-1} nominal resolution, and 1000 scans were co-added to generate spectra with high signal-to-noise ratios.

Fluorescence measurements were performed on a SPEX Fluoromax spectrofluorimeter (Instruments S. A., Edison, NJ) using quartz cuvettes in a thermostated jacket. In fluorescence experiments, an excitation wavelength and a bandwidth of 284 and 3 nm respectively, were selected. Fluorescence resonance energy-transfer (FRET) experiments were carried out using tryptophans of the protein as energy donors and 10 mol % *N*-dansyl-phosphatidylethanolamine (DPE) in phospholipid vesicles as an energy acceptor. The spectra were corrected by subtracting the background spectra, which were measured in the absence of protein.

UV/vis measurements were performed in quartz cuvettes on a Hitachi U-2000 UV/vis spectrophotometer (Hitachi Instruments, Dublin, PA). The absorptions at 234 and 280 nm, corresponding to conjugated dienes and ketodienes, were converted to molar concentrations using extinction coefficients 25 000 and 22 000 M^{-1} cm^{-1}, respectively (*48*, *53*).

RESULTS

Membrane Binding of L-1. Membrane binding of L-1 was demonstrated by ATR FTIR and FRET techniques. Due to the exponentially decaying evanescent field strength, the ATR FTIR absorption spectrum is dominated by the signal from the protein bound to the substrate-supported membrane. The protein molecules in the bulk aqueous phase far from the membrane do not contribute to the signal (*54*). When L-1 was injected to a supported bilayer in the ATR cell, incubated for ∼20 min, and flushed with the buffer, the amide-I band area decreased by only ≤30% (not shown), indicating that L-1 binds to the bilayers. The ∼30% decrease in the amide-I band area was presumably due to the removal of the unbound L-1 from the membrane vicinity. In FRET

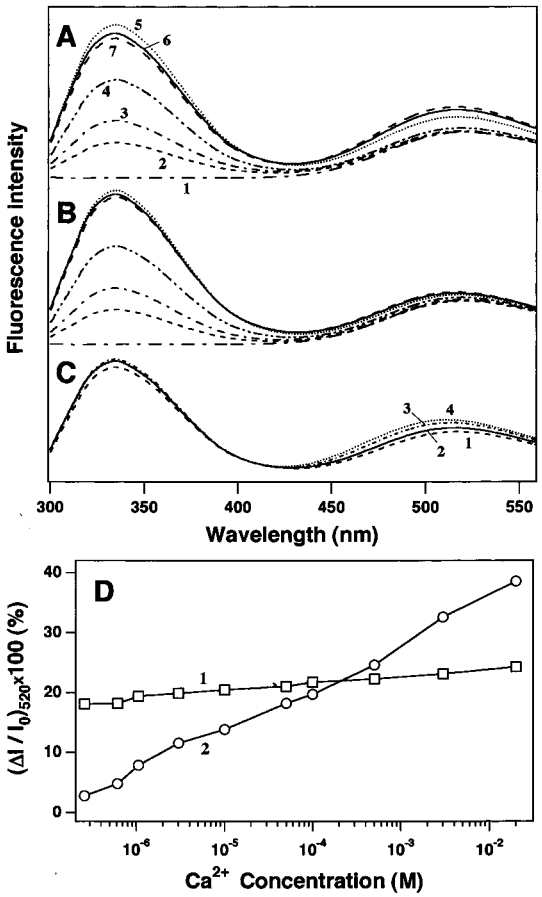

FIGURE 1: Binding of L-1 to phospholipid vesicles composed of 90% POPC + 10% DPE (A) and 70% POPC + 20% POPS + 10% DPE (B, C) as measured by FRET in 50 mM NaCl, 10 μM $CaCl_2$, 10 mM Hepes, and 10 mM Capso (pH 9.0) at 25 °C. The total lipid concentration was 0.2 mM. The curves 1−5 in A and B (the line types and numbers in A and B are the same) correspond to L-1 concentrations of 0, 0.4, 1, 2, and 4 μM, respectively. The spectra 5−7 were measured 1, 6, and 14 min after addition of 4 μM L-1 to phospholipid vesicles. The spectra 1−4 in panel C were measured in the presence of 2.8 μM L-1 and 0.01, 0.1, 1.0, and 10 mM $CaCl_2$, respectively. The effect of $CaCl_2$ on the binding of L-1 to the vesicles without (curve 1) and with 20% POPS (curve 2) is shown in panel D, where $\Delta I = I - I_0$, I and I_0 are the fluorescence emission intensities at 520 nm in the presence and absence of L-1, respectively. The excitation wavelength was 284 nm.

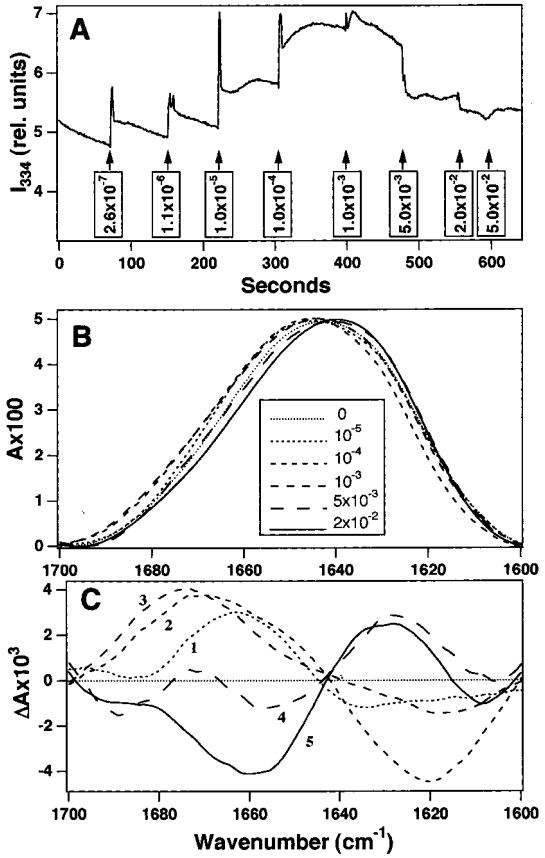

FIGURE 2: Effect of Ca^{2+} on the structure of L-1 as measured by tryptophan fluorescence (A) and FTIR spectroscopy (B, C). (A) Effect of stepwise addition of $CaCl_2$ on the Trp fluorescence of 1.2 μM L-1 measured at 334 nm with excitation at 284 nm. Arrows indicate the time points of addition of $CaCl_2$ at molar concentrations shown in boxes. (B) Infrared amide-I absorption bands of 12 μM L-1 in a D_2O buffer (pH* 8.6) at various molar $CaCl_2$ concentrations, as indicated in the box. (C) Difference spectra, calculated on the basis of the spectra in panel B. The amide-I band in the absence of Ca^{2+} (100 μM EGTA) was subtracted from those in the presence of 0.01−20 mM Ca^{2+} (curves 1−5, respectively). Buffer and temperature are the same as in Figure 1.

experiments, L-1 was added to the vesicles composed of 90% 1-palmitoyl-2-oleoylphosphatidylcholine (POPC) and 10% DPE, which has excitation and emission wavelengths of ∼340 and ∼520 nm, respectively. Excitation of the tryptophans of L-1 at 284 nm resulted in a dose-dependent increase in the DPE fluorescence at ∼520 nm, indicating energy transfer from L-1 to DPE (Figure 1A, curves 1−5). The slope of the dependence of Trp fluorescence emission intensity on L-1 concentration in a double logarithmic scale was significantly lower than 1 (0.64−0.87, lower at higher L-1 concentrations), which is evidently due to the absorption of a fraction (0.13−0.36) of the Trp emission energy by DPE. At a constant concentration of L-1, a time-dependent decrease in the Trp fluorescence at 334 nm was paralleled by an increase in the DPE fluorescence at 520 nm (Figure 1A, curves 5−7). The increase in DPE fluorescence in the presence of L-1 clearly indicates binding of L-1 to the vesicle surface. With membranes containing 20% acidic phospholipid 1-palmitoyl-2-oleoylphosphatidylserine (POPS), the energy transfer was much weaker (Figure 1B), probably owing to electrostatic repulsion between the negatively charged membranes and the acidic protein (pI = 5.85). Interestingly, addition of $CaCl_2$ strongly enhanced the binding of L-1 to negatively charged membranes, but Ca^{2+} was less effective in supporting the binding of L-1 to zwitterionic membranes (Figure 1C,D).

Effect of Ca^{2+} on the Structure of L-1. The data of Figure 1, parts C and D, indicate that Ca^{2+}, while monotonically promoting membrane binding of L-1, has a biphasic effect on the Trp fluorescence. This is confirmed by Figure 2A, which demonstrates that Ca^{2+} at concentrations up to ∼1 mM significantly increases and, at higher concentrations, suppresses the Trp emission intensity of L-1. The quantum yield of Trp is known to increase with decreasing polarity of its microenvironment, which is controlled by the degree of exposure of tryptophans to the polar solvent, water (*55*). Therefore, this result is likely due to a restricted water accessibility to the protein core caused by ≤1 mM Ca^{2+} and increased water accessibility at higher Ca^{2+} concentrations. This was further supported by direct amide hydrogen/deuterium (H/D) exchange experiments performed by FTIR

technique. Amide H/D exchange causes a shift of the amide-I absorption band toward lower frequencies because of heavier nuclear mass of deuterium; the frequency of the vibration of two nuclei in a diatomic molecule is proportional to $(1/m_1 + 1/m_2)^{1/2}$, where m_1 and m_2 are the masses of the two nuclei. The efficiency of amide H/D exchange upon replacement of H_2O by D_2O increases with increasing solvent accessibility to the protein residues. Figure 2B indicates that addition of $CaCl_2$ up to ~1 mM results in a blue shift of the amide-I band of L-1, while at higher Ca^{2+} concentrations the amide-I band is shifted toward lower wavenumbers (wavenumber $= \nu/c$, where ν is the vibrational frequency in s^{-1} and c is the speed of light in cm s^{-1}). The difference spectra shown in Figure 2C demonstrate this effect more clearly. Subtraction of the amide-I band of the protein in the absence of Ca^{2+} (100 μM EGTA) from those in the presence of <1 mM Ca^{2+} yields positive absorption at the higher wavenumbers and negative absorption at the lower wavenumbers, whereas the opposite is true for higher Ca^{2+} concentrations. Thus, fluorescence and FTIR results consistently indicate a biphasic effect of Ca^{2+} on solvent accessibility to the protein body. At concentrations ≤1 mM, Ca^{2+} increases Trp fluorescence of L-1 and causes a shift of the infrared amide-I band of the protein to higher frequencies. The most straightforward interpretation of these effects is that, at this concentration range of Ca^{2+}, the tertiary structure of the protein becomes more compact, or less accessible to water molecules (D_2O in FTIR experiments). This reduces the efficiency of amide H/D exchange, producing amide-I bands at higher frequencies, and renders the protein core less polar, resulting in increased quantum yield of Trp fluorescence. Higher concentrations of Ca^{2+} likely exert the opposite effect; that is, they increase the water accessibility, which accounts for lower-frequency amide-I bands and decreased quantum yield of Trp emission.

Specificity of Ca^{2+} Effects on the Structure and Membrane Binding of L-1. To determine whether the effects of Ca^{2+} ions on the structure and membrane binding of L-1 are specific, we measured the dependence of Trp fluorescence of L-1 and energy transfer from Trp residues of L-1 to DPE in lipid vesicles on the concentration of $MgCl_2$. Magnesium was chosen because it is another physiologically important cation and many Ca^{2+}-dependent cellular events demonstrate Ca^{2+}/Mg^{2+} specificity. The data of Figure 3A show that Mg^{2+} ions have little effect on the Trp fluorescence of L-1. Comparison of the results presented in Figures 2A and 3A clearly indicates a profound specificity of Ca^{2+} ions versus Mg^{2+} ions in affecting Trp fluorescence emission of the protein. Magnesium is also not effective in supporting the binding of L-1 to vesicles containing 20% POPS, as shown in Figure 3B. Although other divalent cations have to be tested to gain more detailed information on the specificity of the effects exerted by Ca^{2+}, which is the subject of our further work, the data of Figure 3 unambiguously demonstrate that the effects of Ca^{2+} on the structure and membrane binding of L-1 are specific.

Effect of Phospholipid Membranes and Fatty Acids on the Structure of L-1. Addition of dioleoylphosphatidylcholine (DOPC) vesicles to L-1 caused a 2.5-nm blue shift, an 18% increase in the quantum yield, and a broadening of the Trp fluorescence spectrum (Figure 4A). The first two effects are probably due to a decreased polarity experienced by the

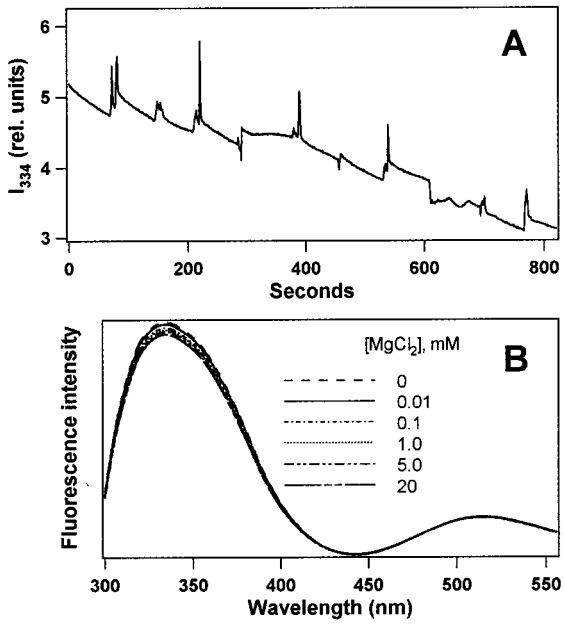

FIGURE 3: Effect of Mg^{2+} on the structure of L-1 as measured by tryptophan fluorescence (A) and on binding of L-1 to vesicles containing 20% POPS (B). (A) Fluorescence emission at 334 nm of 1.2 μM L-1 ($\lambda_{excitation} = 284$ nm). Spikes correspond to additions of $MgCl_2$ at the following concentrations (from left to right): 2.6×10^{-7}, 1.1×10^{-6}, 1×10^{-5}, 1×10^{-4}, 1×10^{-3}, 5×10^{-3}, 2×10^{-2}, 5×10^{-2}, 0.1, and 0.2 M. (B) Fluorescence emission spectra of L-1 in the presence of phospholipid vesicles composed of 70% POPC, 20% POPS, and 10% DPE in the absence and presence of 0.01−20 mM $MgCl_2$, as indicated ($\lambda_{excitation} = 284$ nm). Buffer and temperature are the same as in Figure 1.

indole rings of some of the 14 tryptophans of L-1 upon interactions with membranes. However, the broadening of the Trp emission spectrum indicates an average higher polarity, that is, enhanced access for water to the tryptophans in the protein hydrophobic core (*55*). When vesicles composed of 1-palmitoyl-2-stearoyl(4,5-dibromo)phosphatidylcholine were used, a smaller blue shift and only a weak quenching of Trp fluorescence by bromines were detected, but the fluorescence spectrum was again broadened, suggesting that L-1 binds to these vesicles but the Trp side chains barely reach the bromines at 4,5 positions of membrane lipids.

Phospholipid vesicles and linoleic acid (LA) cause a red shift in the amide-I band of L-1 (Figure 4B), indicating more extensive amide H/D exchange and, consequently, a less compact tertiary structure of L-1. The second derivatives uncover more detailed spectral transformations in the conformation-sensitive amide-I bands (Figure 4C). The major effect is the appearance of a new component at ~1658 cm^{-1} upon interactions of L-1 with the fatty acid or phospholipid, which may be ascribed to α-helices with lower stability (*56*−*58*). These results indicate an overall destabilizing effect of LA micelles and phospholipid bilayers on L-1 which occurs at both the secondary and tertiary structural levels. More specifically, adsorption of L-1 at the surfaces of micelles or membranes induces more open tertiary structure and less stable helices in the protein.

Effects of Ca^{2+} and Interfacial Adsorption of L-1 on Its Activity. To identify the effects of Ca^{2+} and interfacial adsorption of L-1 on the activity of the enzyme, we used UV/vis spectroscopy as a functional assay for L-1. By this

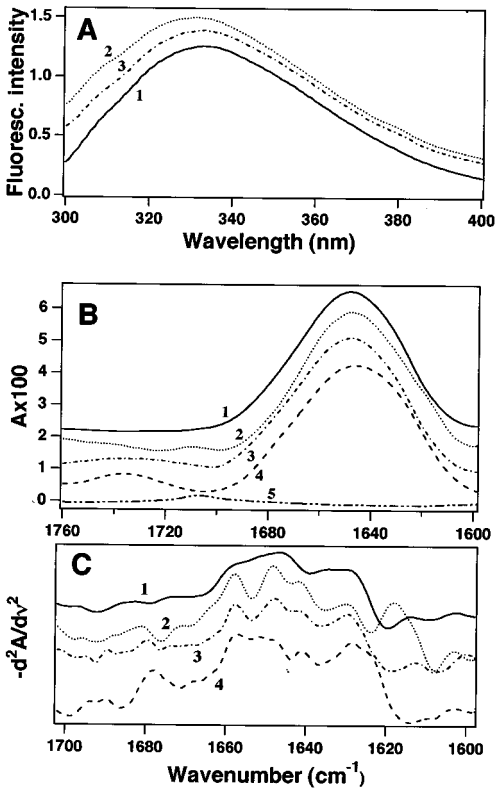

FIGURE 4: Fluorescence and FTIR data indicating structural changes in L-1 induced by membrane binding. In panel A the fluorescence spectra are presented for 0.15 μM L-1 free in solution (1) and in the presence of vesicles (0.6 mM lipid) of DOPC (2) and 1-palmitoyl-2-stearoyl(4,5-dibromo)phosphatidylcholine (3). Curves 1−3 in panel B are the transmittance FTIR spectra of 12 μM free L-1 in solution and in the presence of 4 mM LA and 0.3 mM PLPC, respectively; curve 4 is an ATR spectrum of L-1 bound to a PLPC supported bilayer, and curve 5 is a transmittance spectrum of 5 mM LA. The amide-I band shifts from ~1650 cm^{-1} toward lower frequencies in the presence of lipid or fatty acid. The absorption at ~1707 cm^{-1} (curves 2 and 5) and ~1736 cm^{-1} (curves 3 and 4) in the presence of LA and phospholipids, respectively, is due to their carbonyl stretching vibrations. The second derivatives of the FTIR spectra 1−4 in the amide-I region are shown in panel C. Note the appearance of peaks at ~1658 cm^{-1} in the second derivative spectra 2−4.

method, conjugated dienes (the primary products of polyunsaturated fatty acid hydroperoxidation) and ketodienes (the secondary products) are detected by their characteristic absorption at 234 and 280 nm, respectively (*43*, *48*, *53*). Since binding of L-1 to membranes might be required for hydroperoxidation of fatty acids esterified in membrane lipids, first we determined whether L-1 can utilize esterified LA as a substrate and catalyze its oxygenation. Addition of L-1 to vesicles composed of 1-palmitoyl-2-linoleoylphosphatidylcholine (PLPC), containing esterified LA at the *sn*-2 position, did not cause fatty acid hydroperoxidation, implying that the esterified LA is not a substrate for L-1 (Figure 5A, curve 1). Addition of a secretory PLA_2 in the presence of L-1 resulted in a gradual increase in A_{234}, which was preceded by a lag period of 1−2 min. This lag time is probably necessary for the activation of membrane-bound PLA_2 by a critical amount of the product in the membrane (*59*). When L-1 was added after incubation of PLPC vesicles with PLA_2 for 7−8 min, no lag period was observed in the hydroperoxide production (Figure 5A, curve 2), suggesting that lipid hydrolysis by PLA_2 is the rate-limiting step in eicosanoid biosynthesis. To check whether PLA_2 facilitates hydroperoxidation of LA by liberation of LA from PLPC, thus providing a substrate for L-1, rather than by other (such as structural) effects of PLA_2 on the membrane, we used a covalently modified PLA_2 in which the catalytically important histidine-48 had been bromophenacylated. The absence of absorption at 234 nm in the presence of PLPC, modified PLA_2, and L-1 (Figure 5A, curve 3) indicated that His-48-modified PLA_2 was completely inactive, which is consistent with earlier results (*60*, *61*). These data provide evidence that PLA_2-assisted hydroperoxidation of LA, esterified in PLPC, is due to phospholipid hydrolysis and production of free fatty acid. This procedure, that is, using a system containing PLPC, PLA_2, and lipoxygenase, can be used as a new PLA_2 activity assay. As expected, the generation of conjugated ketodienes was detected at the later stages of catalysis (Figure 5B).

UV/vis spectroscopy was further used to study the dependence of L-1 activity and its mode of action on the aggregation state of the substrate and on Ca^{2+} ions. Figure 6A confirms the data of Figure 5, demonstrating that L-1 does not act on esterified LA at the *sn*-2 position of PLPC, and liberation of LA by PLA_2 in the presence of L-1 is followed by generation of conjugated dienes and conjugated ketodienes, as documented by increased absorption at ~240 and ~280 nm, respectively. These results demonstrate that membrane binding is not associated with the ability of LOXs to utilize lipids as substrate and oxygenate esterified fatty acids, which provides grounds to suggest that membrane binding may be a common feature for all LOXs irrespective of their ability to use esterified fatty acids as substrate. We consistently detect that at LA concentrations below ~1 mM the major L-1 products are conjugated dienes, but at higher LA concentrations the production of conjugated dienes is inhibited and de novo synthesis of conjugated ketodienes is activated (Figure 6B). Above ~1 mM LA the optical density of the solution sharply increases, indicating a transition to a colloidal state (*62*). This result implies that the mode of action of L-1 depends on the aggregation state of the substrate. Free L-1 in solution converts the monodisperse substrate to conjugated dienes, and upon transition of LA to an aggregated micellar state, L-1 catalyzes production of conjugated ketodienes.

Calcium exerts a biphasic effect on the catalytic activity of L-1, which depends on the aggregation state of LA. At 100 μM LA, Ca^{2+} at concentrations <1 mM promotes and at higher concentrations inhibits conjugated diene production with no appreciable generation of conjugated ketodienes (Figure 6C,D). At 2 mM LA, when L-1 catalyzes the synthesis of conjugated ketodienes but not of conjugated dienes, Ca^{2+} at concentrations <1 mM slightly suppresses and at higher concentrations supports conjugated ketodiene production. We conducted similar experiments with suspensions composed of either 100 μM LA + 0.9 mM POPC or 100 μM LA + 0.8 mM POPC + 100 μM 1-palmitoyl-2-lyso-phosphatidylcholine, when most of the fatty acid is in the lipid bilayers or micelles (not shown). The results of these experiments were similar to those with 2 mM, rather than 100 μM, LA indicating that the catalytic mechanism of L-1 is regulated by interfacial adsorption of the enzyme rather than by LA concentration as such. The buffers used in functional assays contained 200 μM dioxygen, and the

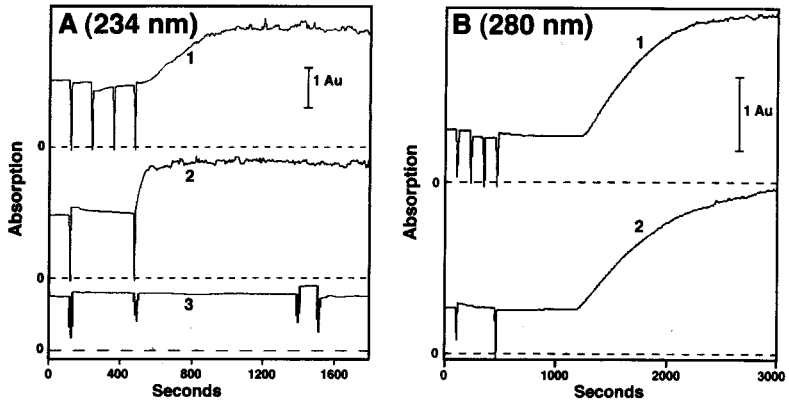

FIGURE 5: UV/vis spectra of 0.3 mM extruded PLPC vesicles in 100 mM NaCl, 5 mM Hepes, pH 8.2, in the time-scan mode. The downward spikes correspond to the following additions to the sample or reference cuvettes (left-to-right): curve 1 in A and B, 50 nM L-1 to reference, 1 μM PLA_2 to reference, 50 nM L-1 to sample, and 1 μM PLA_2 to sample; curve 2 in A and B, 1 μM PLA_2 to sample and 50 nM L-1 to sample (the reference cuvette contains both proteins); curve 3 in A, 1 μM His-48-modified PLA_2 to sample, 50 nM L-1 to sample, 2 μM more modified PLA_2 to sample, and same to reference.

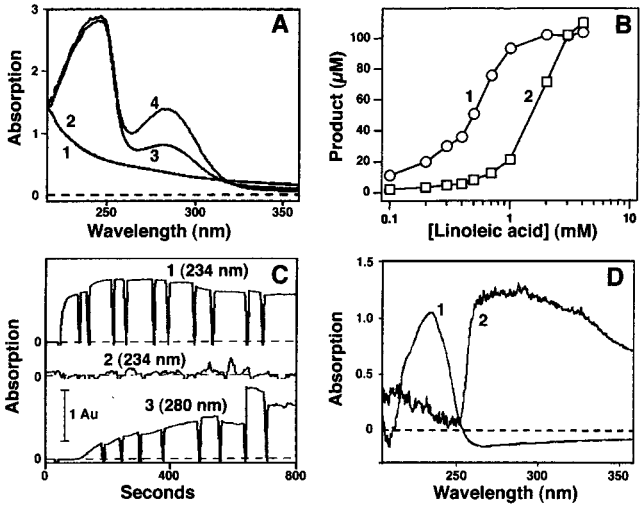

FIGURE 6: (A) UV/vis spectra of 0.5 mM extruded PLPC vesicles in the presence of 50 nM L-1 without (curves 1, 2) and with (curves 3, 4) 1 μM PLA_2 in the wave-scan mode. Spectra 1 and 2 were recorded 32 and 57 min after addition of L-1, and spectra 3 and 4 were recorded 27 and 50 min after addition of PLA_2. L-1 was added to both samples at the same time. The reference cuvette contained 50 nM L-1 (curves 1, 2) or 50 nM L-1 + 1 μM PLA_2 (curves 3, 4). (B) Dependence of the production of conjugated dienes (curve 1) and ketodienes (curve 2) by 50 nM L-1 on LA concentration. (C) Calcium dependence of conversion of 0.1 mM (curve 1) and 2 mM LA (curves 2, 3) to conjugated dienes (curves 1, 2) and ketodienes (curve 3) by 50 nM L-1. The downward spikes indicate additions of L-1 (first addition) and 1 μM, 10 μM, 0.2 mM, 5 mM, and 20 mM $CaCl_2$ (each $CaCl_2$ concentration was first added to the reference and then to the sample cuvette). The last addition of $CaCl_2$ is omitted in curves 3 and 4 because it had little effect. (D) UV/vis spectra of 0.1 mM (curve 1) and 2 mM LA (curve 2) recorded 30 min after addition of 50 nM L-1. The buffer contained 50 mM NaCl, 10 mM Hepes, and 10 mM Capso, pH 8.2 (panel A) and 9.0 (panels B, C, D). In panels B, C, and D the oxygen concentration was adjusted to 200 μM.

samples were bubbled with air after each addition. Therefore the generation of ketodienes could not be interpreted as a result of an anaerobic reaction (*53*).

Possible Mechanism of Ca^{2+} Binding to L-1. Our results provide evidence for a new, Ca^{2+}-regulated membrane-binding mechanism for L-1. In an attempt to find potential Ca^{2+}-binding sites in L-1, we inspected the amino acid sequence and the 3-dimensional high-resolution crystal structure of L-1. Since in Ca^{2+}-binding proteins the cation is usually coordinated by the side chains of acidic residues, we performed a search for Asp and Glu residues that are close enough to each other, either by virtue of the primary sequence or by tertiary folding, to coordinate a Ca^{2+} ion. We found three triads of acidic residues following each other in a row, namely, $Glu^{163}Glu^{164}Glu^{165}$, $Asp^{343}Glu^{344}Glu^{345}$, and $Asp^{636}Asp^{637}Asp^{638}$. The first triad is in the center of α-helix 1, and the spatial configuration of carboxyl oxygens of these residues does not allow them to coordinate a cation (the closest distance of 6.43 Å is found between $O^{\epsilon 2}$ atoms of Glu^{163} and Glu^{164}). The residues 343, 344, and 345 belong to the α-helix 6. The carboxyl oxygens of these residues can hardly ligate a Ca^{2+} ion, because they are separated from each other by ≥6 Å. Although there are several possibilities to position a cation so that it could be coordinated by a combination of carboxyl and carbonyl oxygens, or by the three carbonyl oxygens, these residues cannot be considered as a potential Ca^{2+}-binding site because the mainchain carbonyl groups are involved in helical hydrogen bonding and, additionally, Asp^{343} is involved in a salt bridge with Lys^{483} (*63*). Inspection of the geometry of the third triad, aspartates 636, 637, and 638, showed that these residues cannot coordinate a Ca^{2+} ion for the same reasons as in the preceding case. The next step was to examine the electrostatic surface of the protein. This revealed two potential Ca^{2+}-binding sites, each composed of three acidic residues, namely glutamic acids 21, 106, and 179 (putative Ca^{2+}-binding site I) and Glu^{673}, Asp^{674}, and Glu^{677} (putative Ca^{2+}-binding site II, Figure 7). In each of these two cases, Ca^{2+} can be involved in inner-sphere complexes with two carboxyl groups and in outer-sphere (i.e., through-water) complexes with three to four carboxyl oxygens. In several models of Ca^{2+} binding to these two sites that we have considered, the average distance between Ca^{2+} and protein oxygens was 2.75 ± 0.12 and 2.77 ± 0.02 Å for putative Ca^{2+}-binding sites I and II, respectively. Regarding Ca^{2+}−ligand distances and the presence of only two carboxyl oxygens in the inner coordination sphere of Ca^{2+} (plus a carbonyl oxygen in one model), it is likely that Ca^{2+} binding to L-1 is not strong. We tried to detect protein-bound Ca^{2+} or a lanthanide cation by X-ray crystallography, using crystals grown in the presence of the cations (Dr. Anatoly Kiyatkin, personal communication). However, protein-bound cations were not

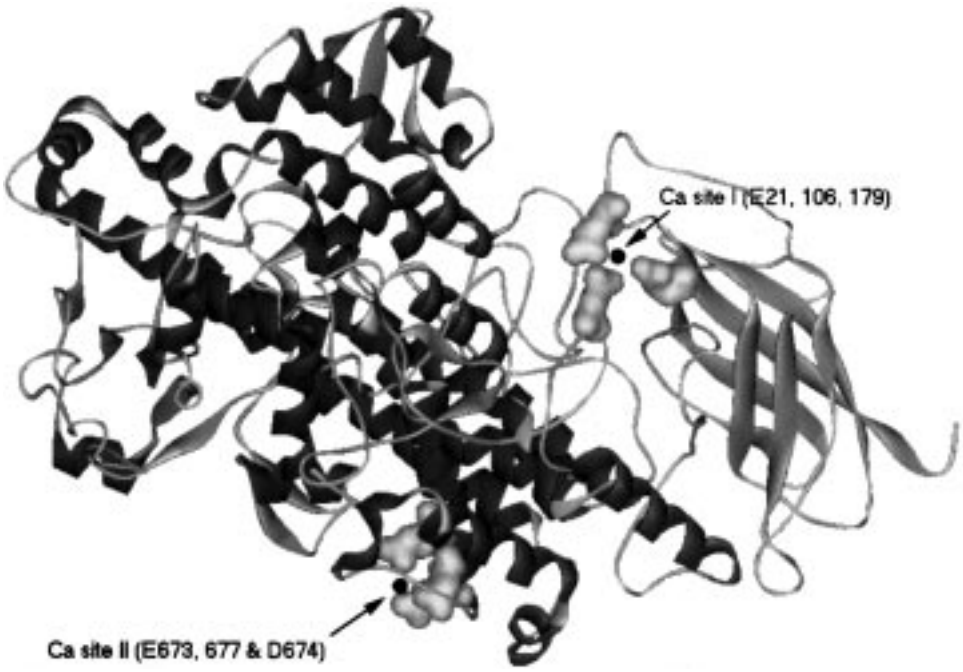

FIGURE 7: A ribbon representation of L-1 structure. van der Waals surfaces of residues Glu^{21}, Glu^{106}, Glu^{179}, Glu^{673}, Asp^{674} and Glu^{677}, constituting the putative Ca^{2+} binding sites I and II, are shown. Two modeled Ca^{2+} ions are placed at putative Ca^{2+} sites I and II and are presented as dark spheres.

detected in these experiments. The most likely reason for this is that L-1 can only be crystallized at acidic pH (pH 5.6); attempts to grow L-1 crystals at neutral pH were not successful. It is both expected and observed experimentally that Ca^{2+} does not bind to some Ca^{2+}-binding motifs in different proteins, such as EF hands of phospholipase C-δ1 (*64*) and troponin C (*65*), because of the acidic pH of the crystal growth medium. At low pH the carboxyl groups are partially protonated and their cation coordination capabilities are weakened.

DISCUSSION

In this work, we provide the first evidence that soybean lipoxygenase-1 binds to phospholipid membranes and that Ca^{2+} ions significantly support the binding of L-1 to negatively charged membranes. In addition, we demonstrate that Ca^{2+} ions and the binding of L-1 to membranes or aggregated substrate affect both the structure and the function of the enzyme. Although in the absence of Ca^{2+} L-1 binds to zwitterionic membranes more effectively than to membranes containing acidic lipids, Ca^{2+} supports L-1 binding to negatively charged membranes and has little effect on L-1 binding to zwitterionic membranes. Calcium ions could facilitate L-1 binding to membranes containing acidic lipids by different mechanisms. First, Ca^{2+} could induce exposure of hydrophobic residues of L-1 that would insert into the membrane core. Second, Ca^{2+} could bind to acidic lipids in the membrane, leading to the neutralization of the negative charge of bilayers and to the elimination of the electrostatic repulsion between the membrane and the protein. Third, Ca^{2+} could form ionic bridges between the negatively charged lipids and the acidic side chains of L-1. The first mechanism can be rejected because in this case Ca^{2+} should have supported protein binding to both zwitterionic and acidic membranes. The second mechanism is hardly feasible because (a) neutralization of the negative charge of the membranes could not support significantly more effective L-1 binding as compared to zwitterionic membranes, and (b) Ca^{2+} is known to neutralize the negative surface charge of membranes containing phosphatidylserine only at $[Ca^{2+}]$ $\sim$0.1 M (*66*), whereas Ca^{2+}-promoted binding of L-1 to the vesicles containing POPS reaches the level of the binding to POPC membranes at Ca^{2+} concentrations of $\sim$0.2 mM (Figure 1D). These considerations imply that the most likely mechanism of the Ca^{2+}-mediated membrane binding of L-1 is that Ca^{2+} ions form salt bridges between the acidic residues of L-1 and the negatively charged lipids in the membrane, although a combination of this and the other two mechanisms cannot be ruled out.

Since Ca^{2+} promotes the binding of L-1 to acidic membranes, we tried to find structural and sequence similarities between potential Ca^{2+} binding sites of L-1 and specific sequences in other proteins involved in Ca^{2+}-mediated membrane binding, such as the Ca^{2+}-dependent lipid-binding (CaLB) domains identified in cytosolic PLA_2s, synaptotagmin, various isoforms of phospholipase C, and some other proteins (*67*, *68*). The CaLB (or C2) domains are $\sim$130-residue 8-stranded β-barrels, and Ca^{2+}-binding residues (mainly aspartates) belong to loops between β-strands. The Glu^{21} of L-1 is in the extended loop between β-strands 1 and 2, and Glu^{106} is in a turn between β-strands 5 and 6, while Glu179 is in a loop following the α-helix 1. These features reveal some structural similarity between the putative Ca^{2+}-binding site I of L-1 and C2 domains. Ineffectiveness of Mg^{2+} to support membrane binding of both C2-containing proteins (*68*) and L-1 is another common feature between (the Ca^{2+}-binding motifs of) these proteins. Interestingly, Glu^{21} of L-1 is involved in a sequence LEVNPD, which is similar to the inverse sequence DPYVEL that is conserved in the C2 domain of cytosolic PLA_2 (*68*). By using this similarity, we performed sequence alignment between 15 plant LOXs and 9 C2-containing proteins (aligned sequences

Plant Lipoxygenases (N → C)

Source	Topology	Amino Acid Sequence
SoyL1	(19-31)	ELEVN----------PDGSAVDN
SoyL2	(30-61)	VLDFNSVADLTKG--NVGGLIGTGLNVVGSTLDN
SoyL3	(23-49)	VLDVNSVTSVG-------GIIGQGLDLVGSTLDT
Arabido1	(32-45)	VLDFN----------DFNASFLDR
Barley1	(30-43)	VLDLN----------DFGATIIDG
Cuke1	(53-66)	VLDFT----------EFHSNLLDN
Lentil	(23-56)	VLDINALTAAQSPSGIIGGAFGVVGSIAGSIIDT
Pea1	(26-59)	VLDINALTAIKSPTGIVTGAFGAIGGAIGTVVDT
Peacyto	(26-52)	VLDINSLTTVG-------GVIGQGFDILGSTVDN
Peaseed	(26-57)	VLDFNTIVSIGGG--NVHGVIDSGINIIGSTLDG
PotatA	(44-57)	CLDLT----------NVGASLLDR
PotatB	(30-43)	VLDFT----------DLAGSLTGK
Tobac1	(30-43)	VLDFT----------DINASVLDG
Tomat1	(30-43)	ALDFT----------DLAGSLTDK
Tomat2	(30-43)	VLDFI----------NIGASVVDG

C2 Domains (C ← N)

$cPLA_2$	(49-37)	FLEVY----------PDPTDLMD
PLC-γ1	(1115-1103)	EIEVF----------PCVIGRGN
PLC-γ2	(1088-1076)	EVEVF----------PCAISRGL
PLC-β1	(700-690)	DVEVY----------TGVKKD--
PLC-β2	(702-692)	ELEVY----------TRVSRE--
PLC-β3	(732-722)	DVEVY----------IGVKRD--
PLC-β4	(726-716)	DVEVY----------TGIKKD--
PLC-δ1	(659-647)	EVTVK----------PDVISNKN
SynI	(184-172)	FVKVY----------PDSTGGMD

FIGURE 8: Comparison of aligned sequences of fragments of 15 plant lipoxygenases with 9 inverse sequences taken from C2 domains of different proteins. Single-letter codes for amino acids are used. Dashes are introduced to maximize sequence alignment. Boldface letters are used to indicate residues corresponding to Glu^{21} of soybean lipoxygenase-1. The abbreviations for plant lipoxygenase sources are taken from Skrzypczak-Jankun, E., Amzel, L. M., Kroa, B. A., and Funk, M. O., Jr. (1997) *Proteins: Struct., Funct., Genet. 29*, 15−31, and those for C2-containing proteins are from Nalefski, E. A., and Falke, J. J. (1996) *Protein Sci. 5*, 2375−2390.

of 20 plant and 13 mammalian LOXs were kindly provided by Dr. Ewa Skrzypczak-Jankun of the Department of Chemistry, University of Toledo, OH). According to this alignment, Glu^{21} of L-1 is presented by Asp in plant LOXs and is conserved in 6 out of 7 phospholipases C and in cytosolic PLA_2 (Figure 8). The flanking Leu and Val residues are either conserved or replaced by other hydrophobic residues in all 24 sequences presented in Figure 8. If Ca^{2+} supports the interaction of L-1 with membranes by forming an ionic bridge between membrane phospholipids and acidic residues of L-1, including Glu^{21}, the two flanking hydrophobic residues may further reinforce membrane binding of L-1 by inserting their nonpolar side chains into the membrane. We checked whether the other acidic residues involved in putative Ca^{2+}-binding sites I and II are conserved in other LOXs and whether any sequence homology around these residues can be found compared to C2 domains. Although no primary structure similarities were found comparing sequences around these residues with C2 domains, all six residues involved in putative Ca^{2+} sites I and II appeared to be either conserved or substituted by the other acidic residue in 55%−90% (70%−90% if Glu^{673} is left out) of 20 plant LOXs. Comparison with 13 mammalian LOXs revealed a much lower degree of similarity.

Tryptophan side chains are known to strongly promote hydrophobic interactions of membrane proteins with the membrane core (*69*). On the other hand, the Trp fluorescence of L-1 was slightly quenched by the bromines upon its binding to vesicles composed of a phospholipid with two bromines at the 4,5 positions of the *sn*-2 acyl chain, which indicates that Trp side chains barely reach the 4,5 position of the lipid acyl chains. Altogether, our results indicate that L-1 binds to membranes peripherally, involving both hydrophobic and ionic factors.

Binding of Ca^{2+} to the putative Ca^{2+} binding site I is likely to have significant effect on the structure of L-1. This site is composed of two residues belonging to the N-domain of L-1 (Glu^{21} and Glu^{106}) and one residue in the C-domain (Glu^{179}). Incorporation of a Ca^{2+} ion into this site is likely to cause attraction between the loosely connected N-domain and C-domain due to ionic bridging between the carboxyl groups and, thus, lead to a somewhat more compact structure of L-1. This is in accord with our observation that Ca^{2+} at concentrations up to 1 mM decreases solvent accessibility to L-1. Although the effect of higher concentrations of Ca^{2+}, as well as the structural/functional significance of the putative Ca^{2+}-binding site II, still remains unclear, our findings suggest that the N-domain of L-1, whose function has not yet been determined, may be involved in a Ca^{2+}-mediated membrane binding of L-1. We used the sequence alignment and the crystal structure of soybean L-3 enzyme (*38*) to check whether a similar putative Ca^{2+}-binding site can be found

in this protein. The L-3 residues Asp^{25}, Glu^{124}, and Glu^{197} correspond to glutamic acids 21, 106, and 179 of L-1 that are involved in the putative Ca^{2+}-binding site I. Although Asp^{25} in the crystal structure of L-3 is relatively far from Glu^{124} and Glu^{197} (distances between carboxyl oxygens range from 6.97 to 8.78 Å), the configuration of the latter two residues allows the positioning of a cation which is coordinated by both carboxyl oxygens of Glu^{124} and by the $O^{\epsilon 1}$ oxygen of Glu^{197}. These results imply that Ca^{2+} ions may exert similar effects on other plant LOXs.

Our results indicate that Ca^{2+} ions, in addition to supporting the binding of L-1 to negatively charged membranes, exert a biphasic effect on the structure and the activity of L-1; moderate concentrations of Ca^{2+} stabilize L-1 structure and stimulate hydroperoxidation of monodisperse fatty acids, whereas >1 mM Ca^{2+} exerts a destabilizing effect on L-1 structure, which likely occurs at both secondary and tertiary structural levels, and promotes conversion of the fatty acid to conjugated ketodienes. These results radically change the current views on plant LOXs and open new prospects in the structure/function relationship of these enzymes. Plant LOXs may employ a Ca^{2+}-regulated membrane-binding mechanism, which is probably a common feature for both animal and plant LOXs.

In experiments using PLPC vesicles, a secretory PLA_2, and L-1, we demonstrated that liberation of LA by PLA_2 was necessary for providing a substrate for L-1, and that the lipid hydrolysis was the rate-limiting step in the whole process of fatty acid oxygenation. This sequence of events is somewhat similar to the cooperation between cytosolic PLA_2, 5-LOX, and 5-LAP in mammalian cells, as described above. Plant cell signaling involves a transient increase in the cytosolic Ca^{2+} concentration and activation of PLA_2, which is followed by LOX-catalyzed biosynthesis of lipid-derived mediators such as jasmonic acid (*30*−*33*). Our results suggest that the increase in cytosolic Ca^{2+}concentration in plant tissue is likely to trigger partitioning of lipoxygenase from the cytosol to intracellular membranes. This translocation would facilitate the interaction of L-1 with the fatty acid, liberated by PLA_2, and its oxygenation. Remarkably, jasmonic acid, the end product of the action of L-1 on linolenic acid, contains a keto group, but no hydroperoxy groups. Therefore, our finding that Ca^{2+}-regulated membrane binding of L-1 changes its catalytic activity toward the generation of keto compounds seems physiologically relevant because it may facilitate production of jasmonic acid by circumventing intermediate steps.

ACKNOWLEDGMENT

We are grateful to Dr. Rodney L. Biltonen for the generous gift of the native and modified PLA_2, to Dr. Ewa Skrzypczak-Jankun for sending us aligned sequences of LOXs, and to Dr. Krzysztof Lewinski for fruitful discussions. Preparation of Figures 5 and 6 by Jama Coartney is gratefully acknowledged.

REFERENCES

1. Clark, J. D., Schievella, A. R., Nalefski, E. A., and Lin, L.-L (1995) *J. Lipid Mediators Cell Signalling 12*, 83−117.
2. Kramer, R. M., and Sharp, J. D. (1997) *FEBS Lett. 410*, 49−53.
3. Lewis, B. A., Austen, K. F., and Soberman, R. J. (1990) *N. Engl. J. Med. 323*, 645−655.
4. Holtzman, M. J. (1991) *Am. Rev. Respir. Dis. 143*, 188−203.
5. Piomelli, D. (1993) *Curr. Opin. Cell Biol. 5*, 274−280.
6. Harder, D. R., Campbell, W. B., and Roman, R. J. (1995) *J. Vasc. Res. 32*, 79−92.
7. Lupulescu, A. (1996) *Prostaglandins Leukotrienes Essent. Fatty Acids 54*, 83−94.
8. Tsujii, M., Kawano, S., and DuBois, R. N. (1997) *Proc. Natl. Acad. Sci. U.S.A. 94*, 3336−3340.
9. Dahlén, S.-E., and Serhan, C. N. (1991) in *Lipoxygenases and Their Products* (Crooke, S. T., and Wong, A., Eds.) pp 235−276, Academic Press, San Diego, CA.
10. Henderson, W. R., Jr. (1994) *Ann. Intern. Med. 121*, 684−697.
11. Yang, V. W. (1996) *Gastroenterol. Clin. North Am. 25*, 317−332.
12. Badr, K. F. (1997) *Curr. Opin. Nephrol. Hypertension 6*, 111−118.
13. Spector, S. L. (1997) *Drugs 54*, 369−384.
14. Liagre, B., Vergne, P., Rigaud, M., and Beneytout, J. L. (1997) *FEBS Lett. 414*, 159−164.
15. Negro, J. M., Miralles, J. C., Ortiz, J. L., Funes, E., and García. A. (1997) *Allergol. Immunopathol. 25*, 104−112.
16. Kühn, H., and Chan, L. (1997) *Curr. Opin. Lipidol. 8*, 111−117.
17. Koshino, T., Takano, S., Houjo, T., Sano, Y., Kudo, K., Kihara, H., Kitani, S., Takaishi, T., Hirai, K., Ito, K., and Morita, Y. (1998) *Biochem. Biophys. Res. Commun. 247*, 510−513.
18. Tang, D. G., Chen, Y. Q., and Honn, K. V. (1996) *Proc. Natl. Acad. Sci. U.S.A. 93*, 5241−5246.
19. Hofmanová, J., Musilová, E., and Kozubík, A. (1996) *Gen. Physiol. Biophys. 15*, 317−331.
20. Ghosh, J., and Myers, C. E. (1997) *Biochem. Biophys. Res. Commun. 235*, 418−423.
21. Natarajan, R., Esworthy, R., Bai, W., Gu, J.-L., Wilczynski, S., and Nadler, J. (1997) *J. Clin. Endocrinol. Metab. 82*, 1790−1798.
22. Rouzer, C. A., and Kargman, S. (1988) *J. Biol. Chem. 263*, 10980−10988.
23. Abramovitz, M., Wong, E., Cox, M. E., Richardson, C. D., Li, C., and Vickers, P. J. (1993) *Eur. J. Biochem. 215*, 105−111.
24. Pouliot, M., McDonald, P. P., Krump, E., Mancini, J. A., McColl, S. R., Weech, P. K., and Borgeat, P. (1996) *Eur. J. Biochem. 238*, 250−258.
25. Watson, A., and Doherty, F. J. (1994) *Biochem. J. 298*, 377−383.
26. Baba, A., Sakuma, S., Okamoto, H., Inoue, T., and Iwata, H. (1989) *J. Biol. Chem. 264*, 15790−15795.
27. Noguchi, M., Miyano, M., Matsumoto, T., and Noma, M. (1994) *Biochim. Biophys. Acta 1215*, 300−306.
28. Veldink, G. A., Vliegenthart, J. F. G., and Boldingh, J. (1977) *Prog. Chem. Fats Other Lipids 15*, 131−166.
29. Shibata, D., and Axelrod, B. (1995) *J. Lipid Mediators Cell Signalling 12*, 213−228.
30. McAinsh, M. R., Brownlee, C., and Hetherington, A. M. (1990) *Nature 343*, 186−188.
31. Knight, M. R., Campbell, A. K., Smith, S. M., and Trewavas, A. J. (1991) *Nature 352*, 524−526.
32. Scherer, G. F. E. (1994) *Symp. Soc. Exp. Biol. 48*, 229−242.
33. Blechert, S., Brodschelm, W., Hölder, S., Kammerer, L., Kutchan, T. M., Mueller, M. J., Xia, Z.-Q., and Zenk, M. H. (1995) *Proc. Natl. Acad. Sci. U.S.A. 92*, 4099−4105.
34. Theorell, H., Bergström, S., and Åkeson, Å. (1946) *Pharm. Acta Helv. 21*, 318−324.
35. Theorell, H., Holman, R. T., and Åkeson, Å. (1947) *Acta Chem. Scand. 1*, 571−576.
36. Boyington, J. C., Gaffney, B. J., and Amzel, L. M. (1993) *Science 260*, 1482−1486.
37. Minor, W., Steczko, J., Stec, B., Otwinowski, Z., Bolin, J. T., Walter, R., and Axelrod, B. (1996) *Biochemistry 35*, 10687−10701.

38. Skrzypczak-Jankun, E., Amzel, L. M., Kroa, B. A., and Funk, M. O., Jr. (1997) *Proteins: Struct., Funct., Genet. 29*, 15−31.
39. Prigge, S. T., Boyington, J. C., Gaffney, B. J., and Amzel, L. M. (1996) *Proteins: Struct., Funct., Genet. 24*, 275−291.
40. Funk, C. D. (1996) *Biochim. Biophys. Acta 1304*, 65−84.
41. Gillmor, S. A., Villaseñor, A., Fletterick, R., Sigal., E., and Browner, M. F. (1997) *Nat. Struct. Biol. 4*, 1003−1009.
42. Koch, R. B., Brumfliel, B. L., and Brumfliel, M. N. (1971) *J. Am. Oil Chem. Soc. 48*, 532−538.
43. Axelrod, B., Cheesbrough, T. M., and Laakso, S. (1981) *Methods Enzymol. 71*, 441−451.
44. Christopher, J. P., Pistorius, E. K., and Axelrod, B. (1972) *Biochim. Biophys. Acta 284*, 54−62.
45. Galpin, J. R., and Allen, J. C. (1977) *Biochim. Biophys. Acta 488*, 392−401.
46. Maccarrone, M., van Aarle, P. G. M., Veldink, G. A., and Vliegenthart, J. F. G. (1994) *Biochim. Biophys. Acta 1190*, 164−169.
47. Feussner, I., Balkenhoh, T. X., Porzel, A., Kühn, H., and Wasternack, C. (1997) *J. Biol. Chem. 272*, 21635−21641.
48. Steczko, J., Donoho, G. A., Dixon, J. E., Sugimoto, T., and Axelrod, B. (1991) *Protein Expression Purif. 2*, 221−227.
49. Maraganore, J. M., Merutka, G., Cho, W., Welches, W., Kézdy, F. J., and Heinrikson, R. L. (1984) *J. Biol. Chem. 259*, 13839−13843.
50. Bradford, M. M. (1976) *Anal. Biochem. 72*, 248−254.
51. Bers, D. M., Patton, C. W., and Nuccitelli, R. (1994) *Methods Cell Biol. 40*, 3−29.
52. Tatulian, S. A., Cortes, D. M., and Perozo, E. (1998) *FEBS Lett. 423*, 205−212.
53. Garssen, G. J., Vliegenthart, J. F. G., and Boldingh, J. (1971) *Biochem. J. 122*, 327−332.
54. Fringeli, U. P. (1993) in *Internal Reflection Spectroscopy. Theory and Applications* (Mirabella, F. M., Jr., Ed.) pp 255−324, Marcel Dekker, New York.
55. Lakowicz, J. R. (1983) *Principles of Fluorescence Spectroscopy*, Plemun Press, New York.
56. Rothschild, K. J., and Clark, N. A. (1979) *Science 204*, 311−312.
57. Dwivedi, A. M., and Krimm, S. (1984) *Biopolymers 2*, 923−943.
58. Tatulian, S. A., Biltonen, R. L., and Tamm, L. K. (1997) *J. Mol. Biol. 268*, 809−815.
59. Burack, W. R., and Biltonen, R. L. (1994) *Chem. Phys. Lipids 73*, 209−222.
60. Volwerk, J. J., Pieterson, W. A., and de Haas, G. H. (1974) *Biochemistry 13*, 1446−1454.
61. Yang, C. C., and King, K. (1980) *Biochim. Biophys. Acta 614*, 373−388.
62. Shinoda, K., Nakagawa, T., Tamamushi, B., and Isemura, T. (1963) *Colloidal Surfactants. Some Physicochemical Properties*, Academic Press, New York and London.
63. Prigge, S. T., Boyington, J. C., Gaffney, B. J., and Amzel, L. M. (1996) in *Lipoxygenase and Lipoxygenase Pathway Enzymes* (Piazza, G., Ed.) pp 1−32, AOCS Press, Champaign, IL.
64. Grobler, J. A., Essen, L.-O., Williams, R. L., and Hurley, J. H. (1996) *Nat. Struct. Biol. 3*, 788−795.
65. Sundaralingam, M., Bergstrom, R., Strasburg, G., Rao, S. T., Roychowdhury, P., Greaser, M., and Wang, B. C. (1985) *Science 227*, 945−948.
66. Tatulian, S. A. (1995) *J. Colloid Interface Sci. 175*, 131−137.
67. Nalefski, E. A., Sultzman, L. A., Martin, D. M., Kriz, R. W., Towler, P. S., Knopf, J. L., and Clark, J. D. (1994) *J. Biol. Chem. 269*, 18239−18249.
68. Nalefski, E. A., and Falke, J. J. (1996) *Protein Sci. 5*, 2375−2390.
69. Wimley, W. C., and White, S. H. (1996) *Nat. Struct. Biol. 3*, 842−848.

BI981062T